DEPARTMENT OF PHYSICS, IIT BOMBAY

Supervised Learning Project

PH303

The Solar Abundance Problem: A Non Diffusive Energy Transport Solution

Manan Seth
190260028
BTech, Engineering Physics

Mentor:
Prof. Vikram Rentala
Department of Physics

November 28, 2021

1 Acknowledgements

Particle physics and astrophysics have fascinated me for quite a long time, and I would like to thank Prof. Vikram Rentala for giving me the opportunity to explore these fields through the Solar Abundance Problem. I am grateful for his guidance and advice, that introduced me to the world of research.

I would also like to thank Siddhant Tripathy, B. Malavika, Aman Avasthi and Eleena Gupta, my team members for this project who have mentored me from the start and helped me out whenever I have been facing issues with patience and enthusiasm.

Contents

2 Abstract

Our understanding of the Sun has vastly improved over the past few decades with the development of detailed theoretical models and our first studies of the solar interior with helioseismic inversion techniques. These two independent methods test our understanding of physics to highly accurate levels. Recent revisions to the solar abundances have put these at conflict, giving rise to the 'solar abundance problem'. In this report, we cover the theory behind the standard solar models, stellar oscillations and the rise of the conflict. We then look at a possible solution to the problem by introducing an alternate mechanism for non - diffusive energy transport in the sun through dark millicharged particles and dark photons.

3 Introduction

The Sun has been a natural observatory for scientific experiments for millennia. Not only does it provide a glimpse into the outside universe, it also acts as an excellent observatory for testing our theories of particle physics, by being able to produce particles of energies much higher than those possible with our best particle accelerators. It has been rigorously studied to constrain the properties of dark matter, and continues to provide new paths to study these elusive particles.

New revisions to the solar abundances have put two independent theories of the Sun at conflict - paving way for new physics. The metallicity of stars play a massive role in their evolution, affecting parameters such as opacity profiles, nuclear reaction rates, temperature gradients etc. The new data provides a lower metallicity value, which shifts the sound speed profile in standard solar models. However, this shifted value does not match the observed sound speed profile obtained by helioseismic inversions. Some other parameters affected by the lower metallicity are surface helium abundance, radius of the tachoclyne and the density profile.

This report will first cover some of the necessary background for this work, starting from major equations of stellar structure. We will then study the dynamic model of solar oscillations and their implications. Next, we will study the solar abundance problem and a possible solution through a mechanism of non-diffusive energy transport in the solar radiative zone. Finally, we will look at a particular model of light dark fermions coupled to hidden photons as a possible physical model to carry out such a non-diffusive energy transport.

4 Modelling the Stellar Structure [2]

4.1 Equations of Stellar Structure

We begin by trying to model the sun by stating some simplifying assumptions leading to some equations, stated without proof.

1. **Spherical Symmetry:** Assuming spherical symmetry allows us to treat various quantities as one-dimensional functions of radius and greatly simplifies calculations
2. **Mass Conservation:** We assume that the rate of mass lost by the sun is negligible compared to the total solar mass, $M_\odot$, over large time frames. This leads to the following equation
$$\frac{dM_r}{dr} = 4\pi r^2 \rho \tag{1}$$
where ρ is the density at r.
3. **Hydrostatic Equilibrium:** This comes from the long term stability of the sun in the form
$$\frac{dP}{dr} = -\frac{GM_r\rho}{r^2} \tag{2}$$
4. **Energy Conservation:** The energy emitted as part of the solar luminosity L must be generated by energy sources within
$$\frac{dL_r}{dr} = 4\pi r^2(\epsilon + \epsilon_{gr} - \epsilon_\nu) \tag{3}$$
Here L_r is the luminosity at r flowing through an infinitesimal shell, ϵ is the energy generated per unit mass per second by nuclear fusion processes, ϵ_{gr} is the energy absorbed or released due to gravitational expansions or contractions, and ϵ_ν is the energy lost to neutrino emission.
5. **Energy Transport:** The temperature gradient in the sun is a handy way to quantify the rate of energy transport in the following equation
$$\frac{dT}{dr} = -\frac{GM_rT}{r^2P}\nabla = -\frac{GM_rT}{r^2P}\frac{d\ln T}{d\ln P} \tag{4}$$
Where ∇ is the dimensionless 'temperature gradient'. This depends on the nature of energy transport - convective or radiative being the dominant modes in the sun.
6. **Schwarzschild Criterion for Convection:** As mentioned, ∇ depends on the mode of energy transport. For radiative energy transport, we have
$$\nabla = \nabla_{rad} = \frac{3}{64\pi\sigma G}\frac{\kappa L_r P}{M_r T^4} \tag{5}$$
Here σ is the Stefan-Boltzman constant, κ is the opacity function and T is the temperature as a function of r.

For convective energy transport, in adiabatic conditions, we have,

$$\nabla_{ad} \equiv (\partial \ln T / \partial \ln P)_s \tag{6}$$

where s is the specific entropy.

Finally, the Schwarzschild Criterion states that we will have convection when

$$\nabla_{\text{rad}} > \nabla_{\text{ad}} \tag{7}$$

7. **Chemical Composition:** Chemical compositions of elements as a function of radius can change with time due to factors such as

   - Nuclear reactions affecting abundance of a particular isotope:

   $$\frac{\partial X_i}{\partial t} = \frac{m_i}{\rho} \left[\sum_j r_{ji} - \sum_k r_{ik} \right] \tag{8}$$

   where X_i is the mass fraction of the isotope in consideration, m_i the respective mass, r_{ji} is the rate of production from element j, and r_{ik} is the rate of conversion to another element or isotope k.

   - Diffusion and gravitational settling, given by

   $$\frac{\partial X_i}{\partial t} = D \nabla^2 X_i \tag{9}$$

   where D is the diffusion parameter

   - The rate at which the average abundance of any species i in the convection zone changes will depend on nuclear reactions in the convection zone, as well as the mass limits of spherical shells of radiative and convective zones.

4.2 Mixing Length Theory

The mixing length theory models energy transport through macroscopic eddies, whose mean free path can be modelled in terms of the mixing length parameter α_{MLT} as

$$l_m = \alpha_{MLT} H_P \tag{10}$$

where $H_P = -dr/d \ln P$ is the pressure scale height.

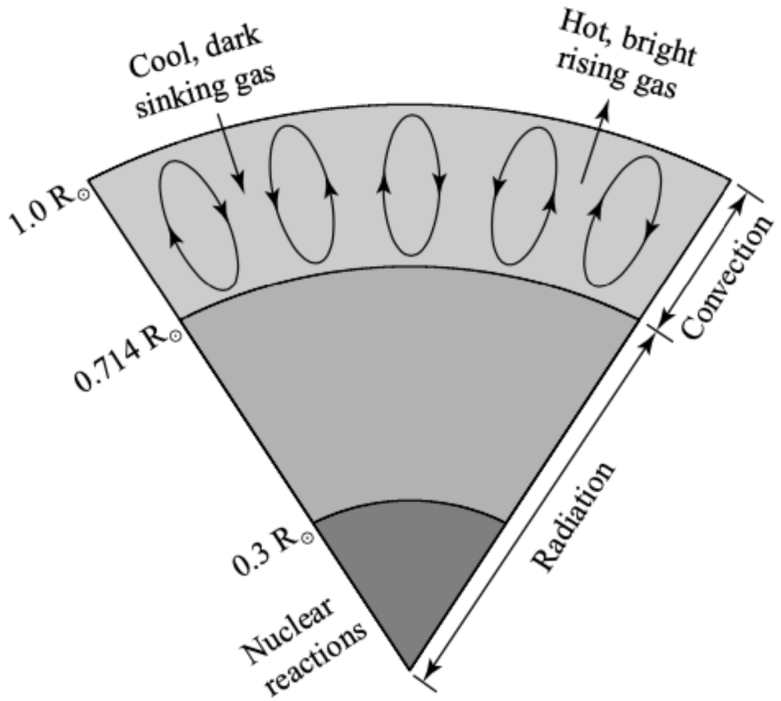

Figure 1: Major layers in the standard solar model [3]

4.3 The Standard Solar Model (SSM) [5]

Until now, we have five unknowns (M_r, ρ, P, L_r and T) and four equations. Thus, we need another equation of state which models the atomic interactions, ionization rates and so on. Popular models of the equation of state are OPAL, MHD and CEFF. This completes our solar model once we provide the following additional parameters:

- **Opacity function** κ: These are generated by modelling inter-particle interactions at various temperatures and densities, and interpolating the singular data points. The OPAL tables are a popular choice for simulated data.
- **Nuclear reaction rates:** We need to provide the nuclear reaction rates, composition changes and neutrino fluxes from a mixture of laboratory measurements and theoretical calculations.
- **Boundary Conditions:** [3]
  as $r \longrightarrow 0 : M_r, L_r \longrightarrow 0$
  as $r \longrightarrow R_* : T, P, \rho \longrightarrow 0$, where R_* is the star's radius.

Standard Solar Models (SSMs) [4] are 1D models for a $1\,M_\odot$ star, starting from a homogeneous model in the pre-main sequence up to the present-day age of the solar system, i.e. $\tau_\odot = 4.57$Gyr. These must follow the following constraints [4]:

- Present-day luminosity $L_\odot = 3.8418 \times 10^{33}$ ers s^{-1}
- Radius $R_\odot = 6.9598 \times 10^{10}$ cm

- $(Z/X)_\odot, Z$ is the metallic abundance and X is hydrogen abundance of the Sun.

The following parameters can be tuned to satisfy the above observational constraints:

- The mixing length parameter α_{MLT}
- Initial helium mass fraction Y_{ini}
- Initial metallicity X_{ini}

Of course we also have a third constraint $X + Y + Z = 1$, where X is the hydrogen mass fraction.

For every model, there are different sources from which $(Z/X)_\odot$ are identified, different equations of state and so on. Thus, different groups have have different standard solar models, and assumptions for each must be carefully studied.

We are now able to model the variables in the solar interior and obtain the following results for a type of SSM:

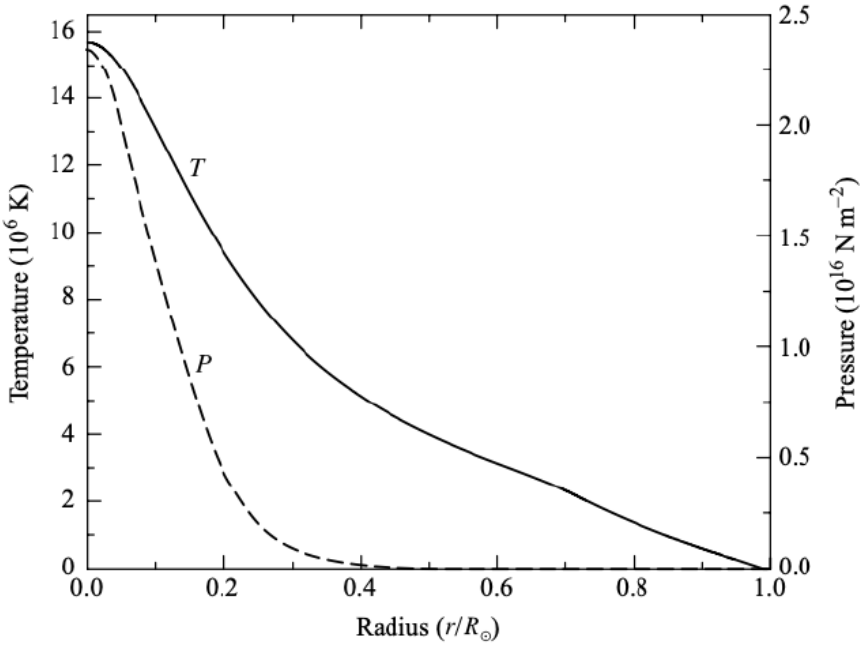

Figure 2: Plot of Temperature T and Pressure P vs r (Data from Bahcall, Pinsonneault, and Basu, Ap. J, 555, 990, 2001.) [3]

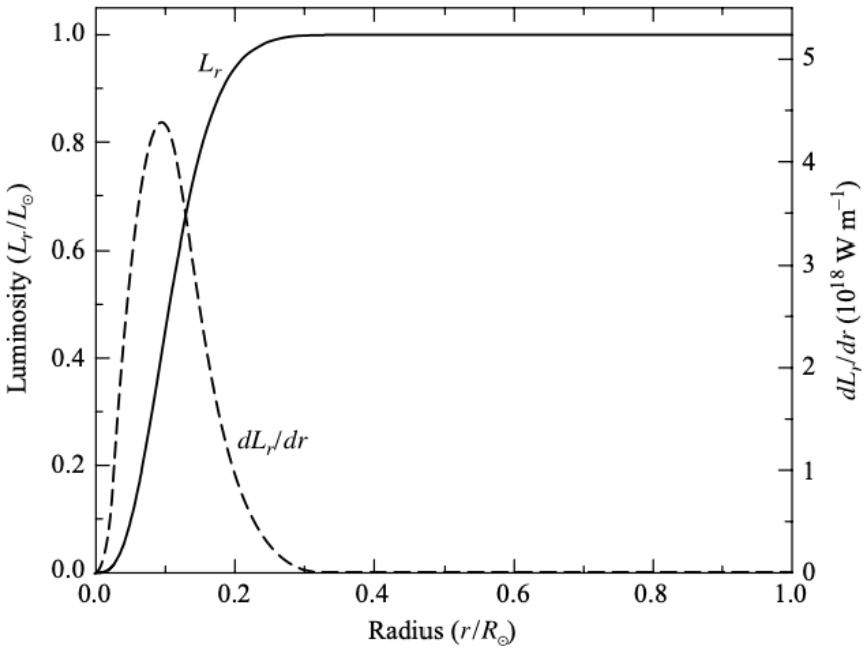

Figure 3: Plot of interior Luminosity profile L_r and its derivative with respect to r, as a function of r (Data from Bahcall, Pinsonneault, and Basu, Ap. J, 555, 990, 2001.) [3]

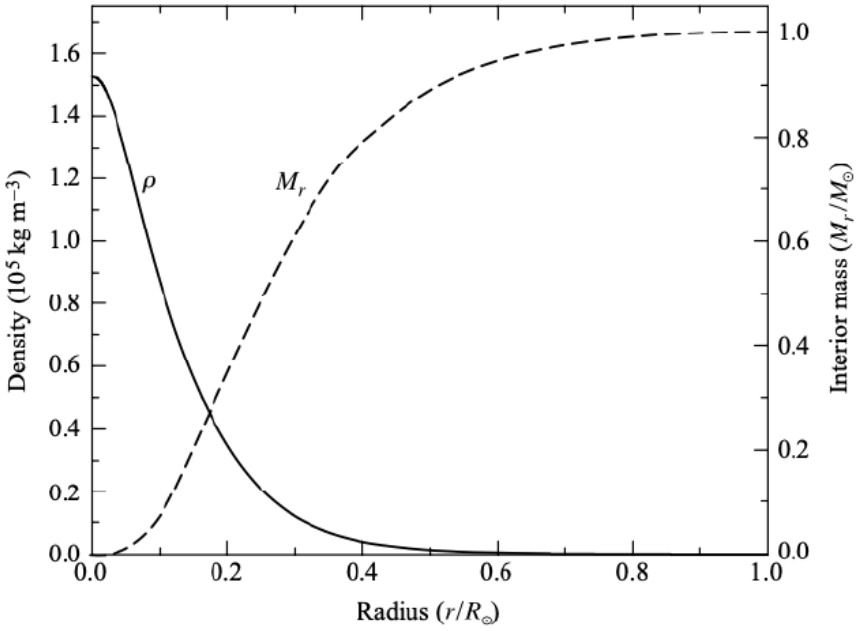

Figure 4: Plot of ρ vs r (Data from Bahcall, Pinsonneault, and Basu, Ap. J, 555, 990, 2001.) [3]

5 Helioseismology [6]

We now study an alternate method to probe the interior of the sun directly through the study of stellar oscillations - helioseismology:

5.1 Equations of Fluid Dynamics

We will model our stellar material as a fluid under the presence of a gravitational potential.

1. **Continuity Equation:**

$$\frac{\partial \rho}{\partial t} + \nabla \cdot (\rho \mathbf{v}) = 0 \tag{11}$$

where $\mathbf{v}$ is the velocity of a fluid element.

2. **Momentum Equation**

$$\rho \left(\frac{\partial \mathbf{v}}{\partial t} + \mathbf{v}.\nabla \mathbf{v} \right) = -\nabla P + \rho \nabla \Phi \tag{12}$$

where Φ is the gravitational potential.

3. **Poisson's Equation**

$$\nabla^2 \Phi = 4\pi G \rho \tag{13}$$

4. **Energy Equation in Adiabatic Approximation**

$$\frac{\partial P}{\partial t} + \mathbf{v}.\nabla P = c_s^2 \left(\frac{\partial \rho}{\partial t} + \mathbf{v}.\nabla \rho \right) \tag{14}$$

where we have the speed of sound

$$c_s = \sqrt{\frac{\Gamma_1 P}{\rho}} \tag{15}$$

where $\Gamma_1 = (\partial \ln P / \partial \ln \rho)_{ad}$.

5.2 Perturbed Form

To study oscillations, we must first perturb the stellar material from it's equilibrium position. For instance, for ρ, we can write

$$\rho(\mathbf{r}, t) = \rho_0(\mathbf{r}) + \rho_1(\mathbf{r}, t) \tag{16}$$

Using the Lagrangian perturbation we have

$$\delta\rho(\mathbf{r}, t) = \rho(\mathbf{r} + \xi(\mathbf{r}, t)) - \rho(\mathbf{r}) = \rho_1(\mathbf{r}, t) + \xi(\mathbf{r}, t) \cdot \nabla \rho_0 \tag{17}$$

where ξ is the displacement from equilibrium position, and velocity is $d\xi/dt$.

Substituting the perturbed quantities in 11, 12, 13, and 14, and keeping only the linear terms in perturbation,

$$\rho_1 + \nabla \cdot \left(\rho_0 \vec{\xi}\right) = 0 \tag{18}$$

$$\rho_0 \frac{\partial^2 \vec{\xi}}{\partial t^2} = -\nabla P_1 + \rho_0 \nabla \Phi_1 + \rho_1 \nabla \Phi_0 \tag{19}$$

$$\nabla^2 \Phi_1 = 4\pi G \rho_1 \tag{20}$$

$$P_1 + \vec{\xi} \cdot \nabla P_0 = c_0^2 \left(\rho_1 + \vec{\xi} \cdot \nabla \rho_0\right) \tag{21}$$

In future references to these equations we drop the subscript 0 for equilibrium quantities and retain only the subscripts for perturbed quantities.

5.3 Spherically Symmetric Solutions

In our case of spherical symmetry, the perturbed equations can be factored into radial (r), tangential (θ, ϕ) and temporal parts. Solutions to the tangential parts are given by the spherical harmonic functions:

$$Y_l^m(\theta, \phi) = \sqrt{\frac{(2l+1)}{4\pi} \frac{(l-m)!}{(l+m)!}} P_l^m(\cos\theta) e^{im\phi} \tag{22}$$

where P_l^m denote the Legendre polynomials. Thus we can write

$$\xi_r(r, \theta, \varphi, t) \equiv \xi_r(r) Y_l^m(\theta, \varphi) \exp(-i\omega t) \tag{23}$$

$$P_1(r, \theta, \varphi, t) \equiv P_1(r) Y_l^m(\theta, \varphi) \exp(-i\omega t) \tag{24}$$

and so on.

Using these in 18 we get

$$\frac{d\xi_r}{dr} = -\left(\frac{2}{r} + \frac{1}{\Gamma_1 P}\frac{dP}{dr}\right)\xi_r + \frac{1}{\rho c^2}\left(\frac{S_l^2}{\omega^2} - 1\right) P_1 - \frac{l(l+1)}{\omega^2 r^2}\Phi_1 \tag{25}$$

$$\frac{dP_1}{dr} = \rho\left(\omega^2 - N^2\right)\xi_r + \frac{1}{\Gamma_1 P}\frac{dP}{dr} P_1 + \rho \frac{d\Phi_1}{dr} \tag{26}$$

$$\frac{1}{r^2}\frac{d}{dr}\left(r^2 \frac{d\Phi_1}{dr}\right) = -4\pi G\left(\frac{P_1}{c^2} + \frac{\rho \xi_r}{g} N^2\right) + \frac{l(l+1)}{r^2}\Phi_1 \tag{27}$$

where we define the *lamb frequency*

$$S_l^2 = \frac{l(l+1)c^2}{r^2} \tag{28}$$

and the *Brunt-Väisälä frequency*:

$$N^2 = g\left(\frac{1}{\Gamma_1 P}\frac{dP}{dr} - \frac{1}{\rho}\frac{d\rho}{dr}\right) \tag{29}$$

Clearly, $N^2 < 0$ gives back the Schwarzschild Criterion.

Since the equations depend only on l, we can label the eigenvalues with same l with a free index n as $\omega_{n,l}$ where n can be any integer. The degree 'l' is related to the horizontal wavelength of the mode and is approximately the number of nodes on the solar surface. The azimuthal order m defines the number of nodes along the equator. Due to spherical symmetry, the nodes of given n, l are degenerate in m. We have

- $n > 0$: acoustic or p modes, as their restoring force is pressure
- $n = 0$: fundamental mode
- $n < 0$: gravity or g modes, as their restoring force is gravity through buoyancy

5.4 Final Oscillatory Form

Now approximating equations 25 onward, we can assert the following simplifications:

- Cowling approximation: perturbation to the gravitational potential Φ_1 can be ignored where $|n|$ and l are large
- We assume that we are looking far away from center (i.e. large l) so $1/r$ terms are neglected,
- We assume that variations in eigenfunctions is more rapid than equilibrium quantities for high $|n|$ oscillations hence terms containing H_P^{-1} can be neglected, where $H_P = -\frac{dr}{d\ln P}$ is the pressure scale height.

Thus we finally get

$$\frac{d^2\xi_r}{dr^2} = K(r)\xi_r \tag{30}$$

where

$$K(r) = \frac{\omega^2}{c^2}\left(1 - \frac{N^2}{\omega^2}\right)\left(\frac{S_l^2}{\omega^2} - 1\right) \tag{31}$$

For the solution to be oscillatory we need the kernel K to be negative. Thus we have

- $\omega^2 < S_l^2$, and $\omega^2 < N^2$: **g** modes - trapped mainly in the core - restoring force is gravity through buoyancy,
- $\omega^2 > S_l^2$, and $\omega^2 > N^2$: **p** modes - generally oscillatory in outer regions restoring force is mainly pressure;

These conditions can be clearly depicted in Figure 6.

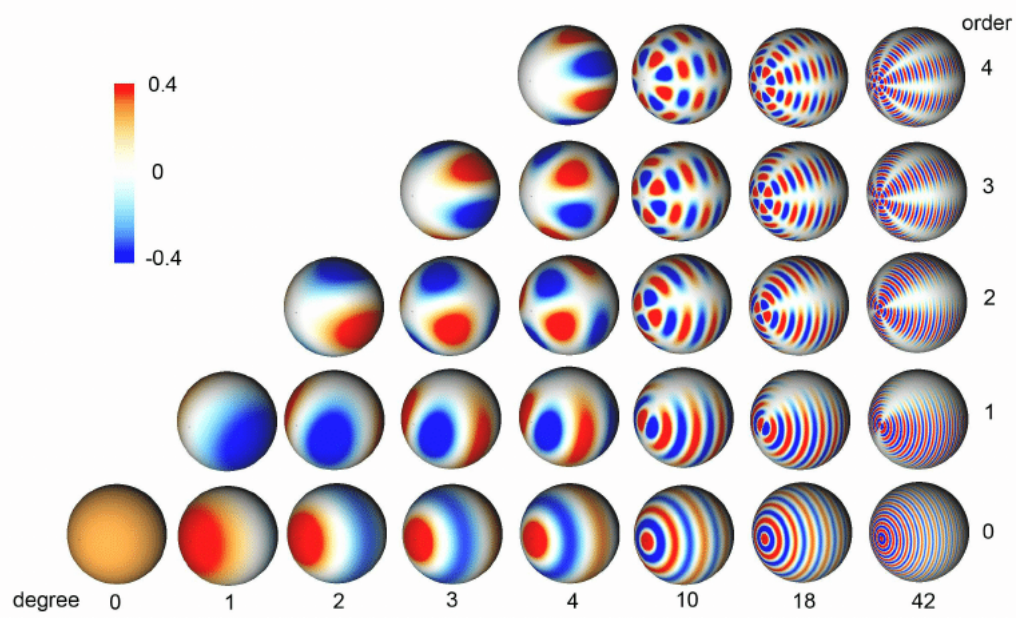

Figure 5: Various spherical harmonics $Y_l^m(\theta,\ \phi)$ [24]

5.5 p modes

The p -modes are trapped between the surface and the inner turning point r_t given by $\omega^2 = S_l^2$. For high frequency p modes, i.e., modes with $\omega \gg N^2$

$$K(r) \simeq \frac{\omega^2 - S_l^2(r)}{c^2(r)} \tag{32}$$

hence, their behavior is predominantly determined by the behavior of the sound-speed profile, which is pressure, i.e., sound waves ($n > 0$).

Figure 10 shows the non-radial p -modes for different degree and order. We observe that lower degree modes penetrate deeper into the core whereas higher degree modes have significant amplitude of oscillation close to the stellar-surface only. Thus, they allow a diagnosis of the conditions on the surface layers.

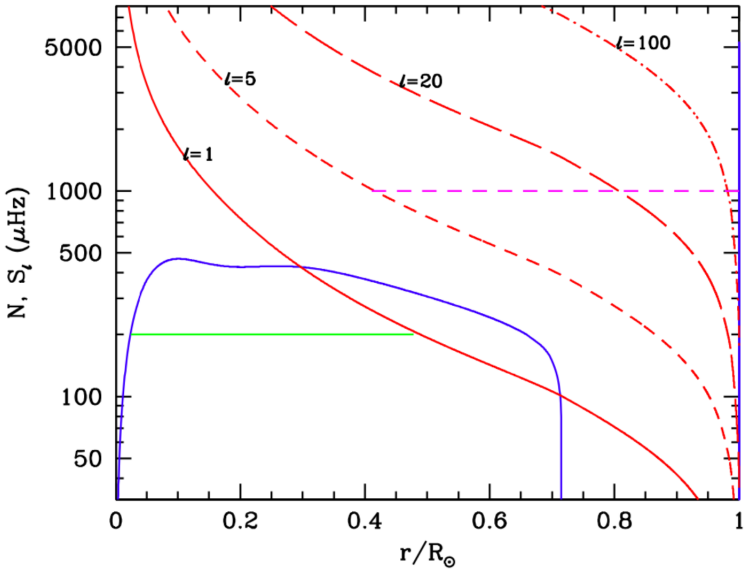

Figure 6: The propagation diagram for a standard solar model. The blue line is the buoyancy frequency, the red lines are the Lamb frequency for different degrees. The green solid horizontal line shows the region where a 200 μHz g-mode can propagate. The pink dashed horizontal line shows where a 1000 μHz l = 5 p-mode can propagate. [8]

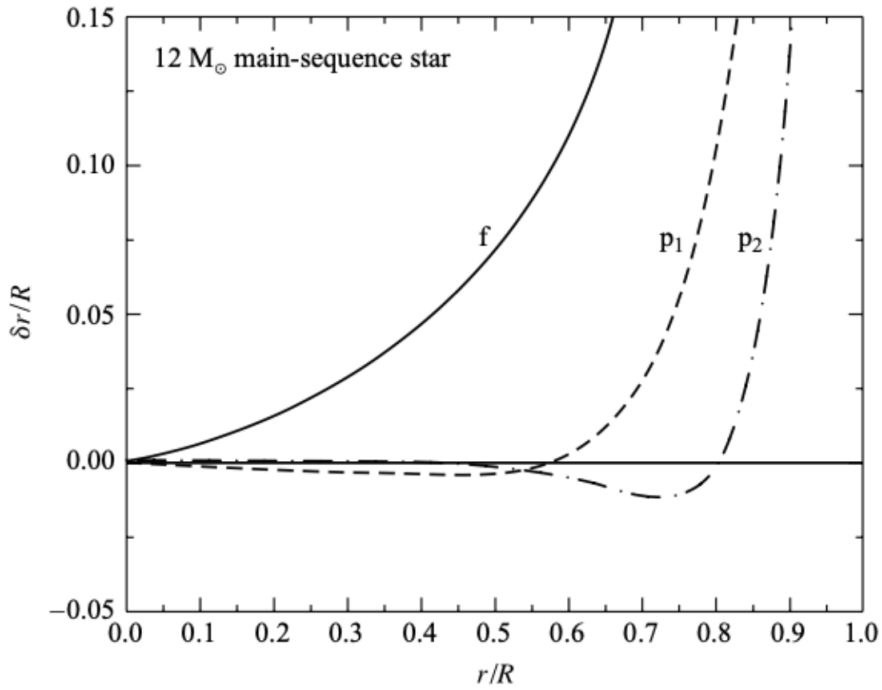

Figure 7: $l = 2$ and f mode is shown for 12 $M_\odot$ star.. [3]

5.6 g modes

In the case of the Sun the g modes are trapped between the base of the convection zone and the core. The turning points of these modes are defined by $N = \omega$. For g -modes of high order, $\omega^2 \ll S_l^2$ and thus

$$K(r) \simeq \frac{1}{\omega^2}\left(N^2 - \omega^2\right)\frac{l(l+1)}{r^2} \tag{33}$$

hence its properties are dominated by the buoyancy frequency N.$(n < 0)$

Now since g modes are trapped deep in the interior, they give us a good idea about the core properties which are essential when we are trying to study the abundances of metals, as well as nuclear reactions. Unfortunately they cannot be directly observed unlike p modes.

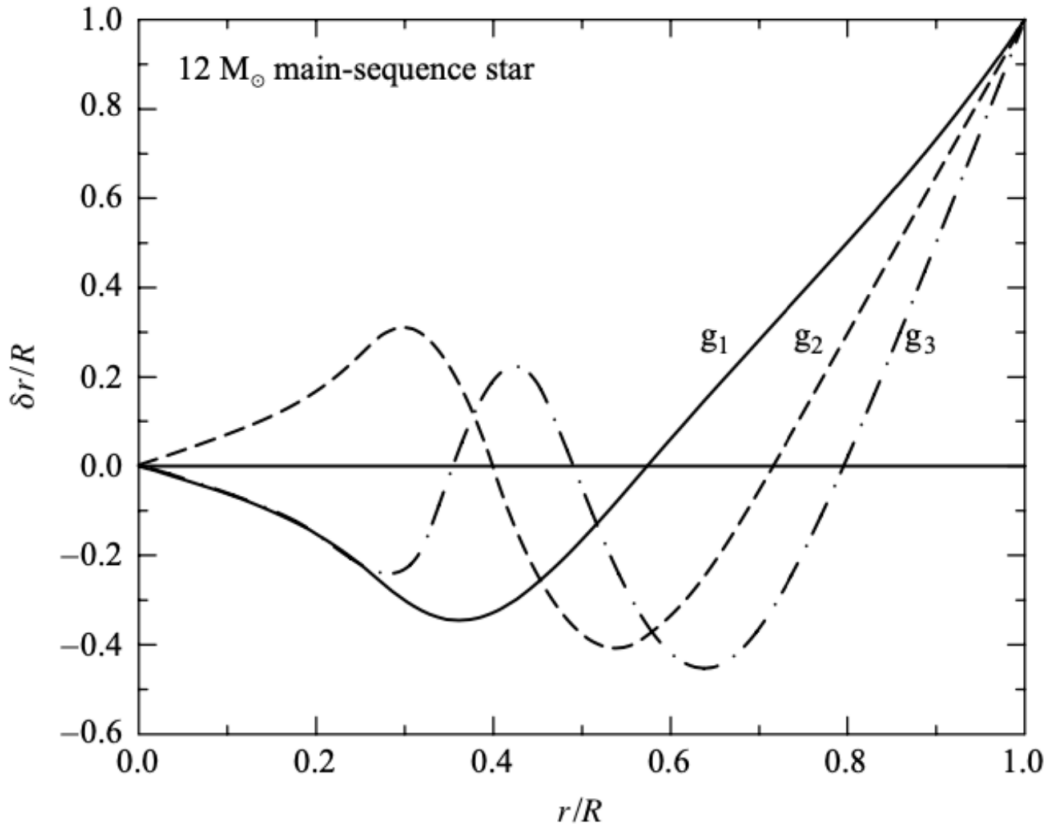

Figure 8: g modes with $l = 2$ [3]

5.7 Helioseismic Inferences

We have 2 main methods for helioseismic inferences:

- **Forward Technique**: Compare frequencies of different models with observed frequencies. For e.g. estimating R_{CZ}- depth of the convection zone

- **Inverse technique**: Using the observed frequencies, infer the internal structure or dynamics. For e.g., sound speed profile $c(r)$.

5.7.1 Helioseismic Inversions [5]

Since the frequencies of acoustic modes depend mainly on the sound speed and density in solar interior, it is possible to invert the frequencies to obtain the sound speed c, and density ρ. It can be shown that c, ρ along with hydrostatic equilibrium are enough to determine the solar model as far as frequencies are concerned. Pressure p and adiabatic index Γ_1 can be determined from c, ρ.

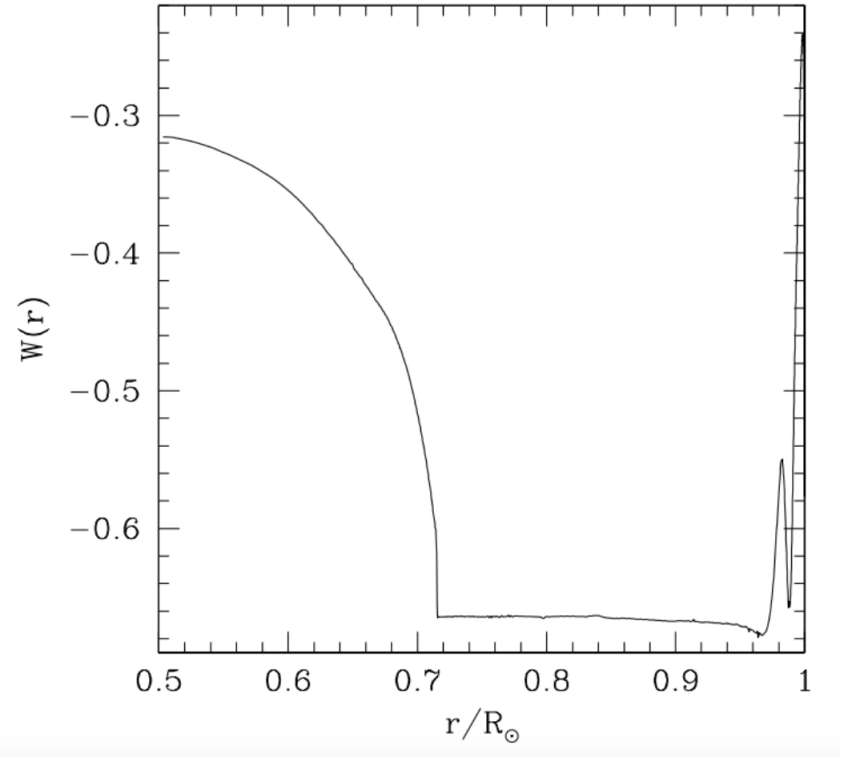

Figure 9: Variation of the dimensionless gradient of sound speed profile $W(r) = \frac{r^2}{Gm}\frac{dc^2}{dr}$ with r. The peak around $r \approx 0.98R_\odot$ is due to the $HeII$ ionization zone and can be calibrated to find helium abundance [5]

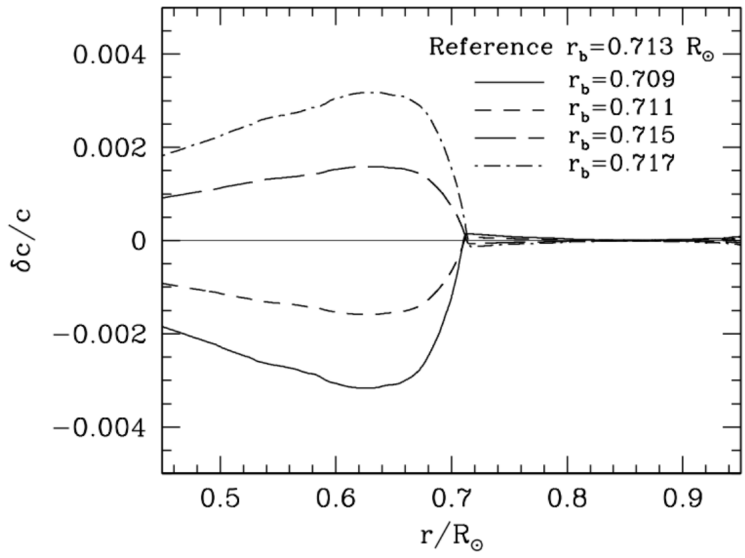

Figure 10: The discontinuity in the sound speed for different models show the position of the tachocline [5]

6 Beyond the Standard Solar Model [21]

As seen earlier, the standard solar model tunes some unknown parameters such as the initial chemical composition, mixing length to fit the known parameters such as solar mass, radius, luminosity etc.
We now rewrite the equations of the standard solar model are:

$$\frac{dP}{dr} = -\frac{GM\rho}{r^2} \tag{34}$$

$$\frac{dM}{dr} = 4\pi r^2 \rho \tag{35}$$

$$\frac{dL}{dr} = 4\pi r^2 \rho \left(\epsilon + \epsilon_{gr} - \epsilon_{\nu}\right) \tag{36}$$

$$\frac{dT}{dr} = -\frac{3\kappa\rho L}{16\pi r^2 \alpha T^3}, \qquad \nabla_{\text{rad}} < \nabla_{\text{ad}} \tag{37}$$

$$= \nabla_{ad} . \frac{T}{P}\frac{dP}{dr}, \qquad \nabla_{\text{rad}} > \nabla_{\text{ad}} \tag{38}$$

$a = 4\sigma$, $\nabla_{ad} = \left(\frac{\partial \ln T}{\partial \ln P}\right)_S$ and $\nabla_{rad} = \frac{3\kappa LP}{16\pi aGMT^4}$. The equation of heat transfer in the core **??** is a form of the Fick's equation
In the convective zone, except in the outermost layers, we can approximate the equation of state as the ideal gas law: $P = \frac{\rho T}{\mu m_H}$, where m_H is the proton mass, μ is mean molecular weight normalized to proton mass, and the Boltzmann constant has been set to unity.

$$\mu = \frac{\Sigma_j n_j A_j}{\Sigma_j n_j (1 + Z_j)} = \left[\Sigma_j \frac{X_j}{A_j}(1 + Z_j)\right]^{-1} \simeq \left[2X + \frac{3Y}{4} + \frac{Z}{2}\right]^{-1} \tag{39}$$

From the ideal gas law and 34, we get

$$T \sim \frac{\mu P}{\rho} \sim \frac{\mu GM}{R} \tag{40}$$

Substituting in 37

$$L \sim \frac{R^2}{\kappa\rho}\left(\frac{T^4}{R}\right) \sim \frac{\mu^4 M^3}{\kappa} \tag{41}$$

Substituting the mean molecular weight,

$$\mu \simeq \frac{4}{8 - 5Y - 6Z} \implies \frac{M^3}{L} \simeq \kappa(8 - 5Y - 6Z)^4 \tag{42}$$

Thus, since the mass and luminosity are fixed, any opacity change must majorly depend on a change in Helium abundance.
The old GS98 model of solar abundances was replaced by the AGSS09 model which better explained the solar spectrum and whose discrepancies with respect to GS98 were well understood. However, the decreased metallicity in AGSS09 dataset gives wrong results with the Standard Solar Model.
As seen earlier, the process of Helioseismic inversion of frequency spectra allows us to gauge the unknown parameters in the Standard Solar model decently accurately, and these conflict with the results from the Standard Solar Model. The main discrepancy is in the sound speed profiles in the solar radiative zone.

7 Non-Diffusive Energy Transport Solution [21]

One of the easiest proposed solutions to the solar abundance problem is to increase the opacity profile in the solar radiative zone.
The non-diffusive energy transport solution considers an analogue of radiative transport, since convective transport in the radiative zone of the sun is inconsistent with Helioseismic data. This can be implemented by emission of some unknown particles from one region of the sun, their propagation/transport in the sun and subsequent energy transfer to another region of the sun.
This will result in additional terms in 36, which may have positive or negative sign.
Shifting from radial to mass coordinates, where primed quantities are mass derivatives:

$$m \equiv M/M_\odot,\ \tilde{r} \equiv r/R_\odot,\ \tilde{\rho} \equiv \rho/\rho_0,\ \tilde{p} \equiv P/P_0,\ \tilde{l} \equiv L/L_\odot,\ \tilde{t} \equiv T/T_0,\ \tilde{\kappa} \equiv \kappa/\kappa_0,\ \tilde{\epsilon} \equiv \epsilon/\epsilon_0$$

where

$$\rho_0 \equiv \frac{M_\odot}{\frac{4}{3}\pi R_\odot^3},\ \ P_0 \equiv \frac{2}{3}\pi R_\odot^2 G\rho_0^2,\ \ T_0 \equiv \frac{GM_\odot m_H}{R_\odot},\ \ \kappa \equiv 1.0\ \ cm^2/g,\ \ \epsilon_0 \equiv 1.0\ \ erg/g.s$$

Rewriting the solar equations in this form:
Hydrostatic equilibrium:

$$p' = -\frac{2m}{3r^4} \tag{43}$$

Continuity equation:

$$r' = \frac{1}{3\rho r^2} \tag{44}$$

Energy production equation:

$$l' = \xi_1 \left(\epsilon_{nuc} - \epsilon_\nu + \sum_i \epsilon_i \right) \tag{45}$$

Energy Transport equation (Fick's Law):

$$t' = -\xi_2 \frac{\kappa l}{r^4 t^3} \tag{46}$$

Equation of state:

$$p = 2\frac{\rho t}{\mu} \tag{47}$$

where the numerical coefficients ξ_1 and ξ_2 are defined as follows:

$$\xi_1 \equiv \epsilon_0 \frac{M_\odot}{L_\odot} \sim 0.52,\ \ \xi_2 \equiv \frac{3}{64\pi^2 a} \frac{\kappa_0 L_\odot M_\odot}{(GM_\odot m_H)^4} \sim 2.4 \times 10^{-5} \tag{48}$$

In 45, the contribution of ϵ_{gr} is small and has been neglected. The terms ϵ_i correspond to non-diffusive energy transport.
In finding the luminous flux power, we can use the constraint of the results which are correct

from the standard solar model. Since the surface luminosity is fixed and has already been characterized by the terms of nuclear emission and neutrino energy losses,

$$\xi_1 \int_0^1 [\epsilon_{nuc}(m) - \epsilon_\nu(m)]_{SSM} dm = 1 \tag{49}$$

where the subscript 'SSM' denotes that the function has been evaluated in the Standard Solar Model's framework.
Finally, we can split the additional terms in the energy production equation as

$$\sum_i \epsilon_i = \sum_i \tilde{\epsilon}_i + \bar{\epsilon}, \quad \bar{\epsilon} \equiv \int_0^1 dm \sum_i \epsilon_i \tag{50}$$

Then by definition $\int_0^1 dm \sum_i \tilde{\epsilon}_i = 0$. This determines the part corresponding to non-diffusive energy transport, and $\bar{\epsilon}$ corresponds to the total power generated in solar plasma by unknown sources or lost by the plasma through unknown sinks.

Let us denote look at any quantity x in the standard solar model, and a model which incorporates an additional energy transport term, and denote the difference in the value of the quantity between the models by δx.
Starting with equations 46 and 43, we get

$$l \propto \frac{mt^3 t'}{\kappa p'} \tag{51}$$

Using the opacity tables such as OPAL, we can write $\kappa \propto \rho^\alpha t^{-\beta}$ for some $\alpha,\ \beta$.
Now using $c_s^2 \propto p/\rho \propto t/\mu$ (where the second proportionality comes from ideal gas law), we get

$$\frac{\delta t}{t} = 2\frac{\delta c_s}{c_s} + \frac{\delta \mu}{\mu} \tag{52}$$

From allowed errors in observed data, we can conclude that the considered variations of density, sound speed, temperature and sound speed profile are much less than unity, validating the approximations of the variational method. Similarly, it can be shown that the variation in p' is much less than unity.
Then, writing t' and p' in terms of helioseismic observables:

$$\frac{\delta t'}{t'} = \frac{(\delta t')}{t'} = \frac{t}{t'}\left(\frac{\delta t}{t}\right)' + \frac{\delta t}{t} = 2\frac{t}{t'}\left(\frac{\delta c_s}{c_s}\right)' + \frac{t}{t'}\left(\frac{\delta \mu}{\mu}\right)' + 2\left(\frac{\delta c_s}{c_s}\right) + \frac{\delta \mu}{\mu} \tag{53}$$

and

$$\frac{\delta p'}{p'} = \frac{p}{p'}\left(\frac{\delta p}{p}\right)' + \frac{\delta p}{p} = \frac{p}{p'}\left(\frac{\delta \rho}{\rho}\right)' + 2\frac{p}{p'}\left(\frac{\delta c_s}{c_s}\right)' + 2\frac{\delta c_s}{c_s} + \frac{\delta \rho}{\rho} \tag{54}$$

Substituting the above results into the solar luminosity variation:

$$\frac{\delta l}{l} = 2(3+\beta)\frac{\delta c_s}{c_s} - (1+\alpha)\frac{\delta \rho}{\rho} + (4+\beta)\frac{\delta \mu}{\mu} + \frac{t}{t'}\left[2\left(\frac{\delta c_s}{c_s}\right)' + \left(\frac{\delta \mu}{\mu}\right)'\right] - \frac{p}{p'}\left[\left(\frac{\delta \rho}{\rho}\right)' + 2\left(\frac{\delta c_s}{c_s}\right)'\right] \tag{55}$$

Since the helioseismic inversions as well as SSM have their errors, it is not straightforward to calculate $\delta l/l$ profile and fix a shape for the required variation. To fix the shape, results from a hypothetical solution of direct variation of opacity is used.

7.1 Model - Direct Opacity Shift [22]

The SSM involves several numerical integration steps of Non-Linear partial differential equations which makes it hard to correctly interpret changes. Thus, the author of [22] paper developed a linear solar model [23] to investigate the role of parameters and assumptions more efficiently.
Take opacity $\kappa(\rho, T, Y, Z_i)$. Consider the effect of metallicity only in the equation of state of the radiative transport in the sun. Then, the AGSS09 metallicity implies a total variation in the opacity profile as:

$$\delta\kappa^{tot}(r) = \frac{\kappa(\rho(r), T(r), Y(r), Z_i(r)}{\bar{\kappa}(\bar{\rho}(r), \bar{T}(r), \bar{Y}(r), \bar{Z}_i(r)} - 1 \tag{56}$$

where the barred terms refer to SSM values, while unbarred terms refer to varied values.
This model will now assume the following

- Performed changes in opacity and heavy element admixture is small
- Variation of chemical composition can be estimated from variation of nuclear reaction rate and diffusion efficiency
- Variation of metal admixture has negligible direct effect on nuclear production of He and on diffusion efficiency

Simplifying the above equation

$$\delta\kappa^{tot}(r) = \kappa_T\delta T(r) + \kappa_\rho\delta\rho(r) + \kappa_Y\Delta Y(r) + \sum_i \kappa_i\delta Z_i(r) + \delta\kappa_I(r) \tag{57}$$

Here, $\delta\kappa_I$ is an intrinsic change in opacity function, and the rest of the terms correspond to the effect of changes in other parameters. The coefficients are:

$$\kappa_T = \frac{\delta \ln \kappa}{\delta \ln T}\|_{SSM} \qquad \kappa_\rho = \frac{\delta \ln \kappa}{\delta \ln \rho}\|_{SSM}$$
$$\kappa_Y = \frac{\delta \ln \kappa}{\delta Y}\|_{SSM} \qquad \kappa_i = \frac{\delta \ln \kappa}{\delta \ln Z_i}\|_{SSM}$$

Now, using the ideal gas equation we can simplify the equation by substituting

$$\delta\rho = \delta P(r) - \delta T(r) - P_Y(r)\Delta Y(r) \tag{58}$$

Where $P_Y(r) = -\frac{\delta \ln \mu}{\delta Y} \simeq -\frac{5}{8-5Y(r)}$. Then substituting the same, and substituting $\delta Z_i(r)$ and $\Delta Y(r)$ from the LSM,

$$\delta\kappa^{tot}(r) = \kappa'_T\delta T(r) + \kappa'_P\delta P(r) + \kappa'_Y\Delta Y_{ini} + \kappa_c\delta C + [\delta\kappa_I(r) + \delta\kappa_Z(r)] \tag{59}$$

κ_Z is the composition opacity change, given by $\delta\kappa_Z(r) = \sum_i \kappa_i\delta z_i$.

$$\kappa'_T = \kappa_T - \kappa_\rho(1 + P_Y\xi_T) - K_Y\xi_T$$
$$\kappa'_P = \kappa_\rho(1 - P_Y\xi_p) - K_Y\xi_P$$
$$\kappa'_Y = (\kappa_Y - \kappa_\rho P_Y)\xi_Y + Q_Y\kappa_Z\kappa_C = Q_C\kappa_Z$$

The coefficients Q_h and ξ_h are given by detailed calculations of the solar composition in the LSM, which is covered in [23].
In 59, the parts not in square brackets [ ] can be derived, however, the part in [ ] can, in principle, be varied in any way. Thus, we must set bounds based on observational data.
Thus, this approach finds variation in opacity based on the equations of state of the solar model, and fitting data to observations. This opacity will differ from the opacity values calculated by OPAL and others, which were derived by theoretical modelling of inter-particle interactions at the various densities and temperatures, which gives singular points which can be interpolated to form functions for the SSM.

Coming back to the luminosity variation, $\bar{\delta}$ refers to variation in the B16 SSM with respect to this shifted opacity model. This gives the final results:

$$(\delta l)_{add} = l\times\left(\frac{\bar{\delta}\kappa}{\kappa} + 2\beta\frac{\delta c_s}{c_s} - \alpha\frac{\delta\rho}{\rho} + \beta\frac{\bar{\delta}\mu}{\mu} + (4+\beta)\left(\frac{\delta\mu}{\mu}\right)_{nuc} + \frac{t}{t'}\left(\frac{\delta\mu}{\mu}\right)'_{nuc} + \left(\frac{\bar{\delta}l - \delta l}{l}\right)_{nuc}\right) \tag{60}$$

Using this, we will discussed the results in case of $\bar{\epsilon} = 0$ and $\bar{\epsilon} \neq 0$

7.2 Results: $\bar{\epsilon} = 0$

In this case,

$$(\delta l)_{nuc} = (\bar{\delta} l)_{nuc} \text{ If } \bar{\epsilon} = 0$$

The sun does not lose or gain any additional energy. Then, 60 simplifies to

$$(\delta l)_{add} = l \times \left(\frac{\bar{\delta}\kappa}{\kappa} + 2\beta\frac{\delta c_s}{c_s} - \alpha\frac{\delta\rho}{\rho} + \beta\frac{\bar{\delta}\mu}{\mu}\right) \tag{61}$$

Here, from 42, we can relate the quantity $\bar{\delta}\mu$ with the helioseismological surface helium abundance. The variation $\bar{\kappa}$ is taken from the reference of section 7.1. Using this opacity and the relations $\kappa \propto \rho^{\alpha} t^{-\beta}$, and $c_s \propto p/\rho \propto t/\mu$, we obtain the remaining terms.
Note that since the formula uses Fick's Law, it is only valid in the radiative zone.
Since the SSM assumes effective convective mixing in the convective zone, and agrees with Helioseismology data, we cannot significantly change the energy transport terms without contradictions.
Thus, according to the plot, we require emission on particles at the boundary of convective zone, and some source of heating within approximately $r \in [0.1, 0.3]$.
If we are interested in reconciliation of sound speed profile (since global rescaling of opacity does not influence it), we can add an arbitrary constant to the RHS of 60. This resembles the solution of the anomaly provided by dark matter diffusive energy transport.
Numerically, the case of C = -0.26 results in the required additional energy transfer from the centre of the solar core to its periphery.

7.3 Results: $\bar{\epsilon} \neq 0$

The additional 3 terms in 60 have been estimated earlier.
The case of $\bar{\epsilon} = -0.2$, which corresponds to maximum allowed energy loss through solar

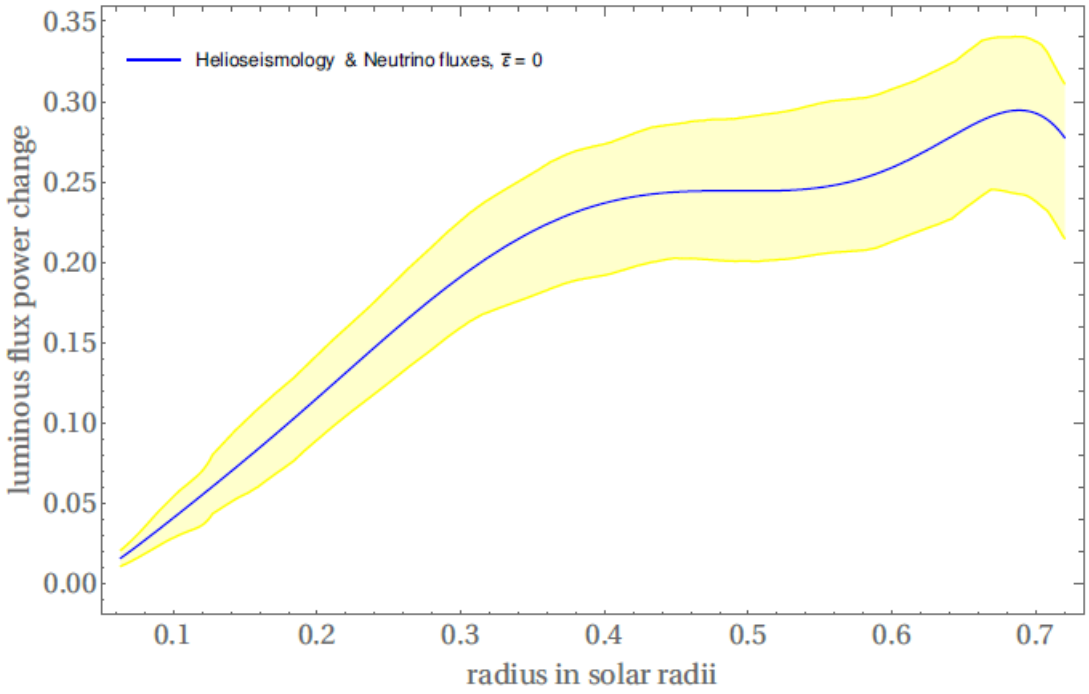

Figure 11: Additional power of luminous flux $(\delta l)_{add}$, which solves the solar abundance problem, as a function of radial coordinate inside the core and radiative zone, $\bar{\epsilon} = 0$ [21]

neutrino data, gives a requirement of the required power being dominantly positive (Fig 13). However, if we were to try to solve the solar abundance problem by loss of energy alone, the additional power profile would need to be non-positive.

Analogously, the case $\bar{\epsilon} > 0$ requires $(\delta l)_{add} > 0.2$, whereas the solar neutrino data allows a maximum $l_{gain} < 0.1$. Thus, although some limited loss or gain of energy by the Sun is allowed in principle, the resulting addition to the power profile becomes wavy in the core, making it hard to find a real physical model to explain the same.

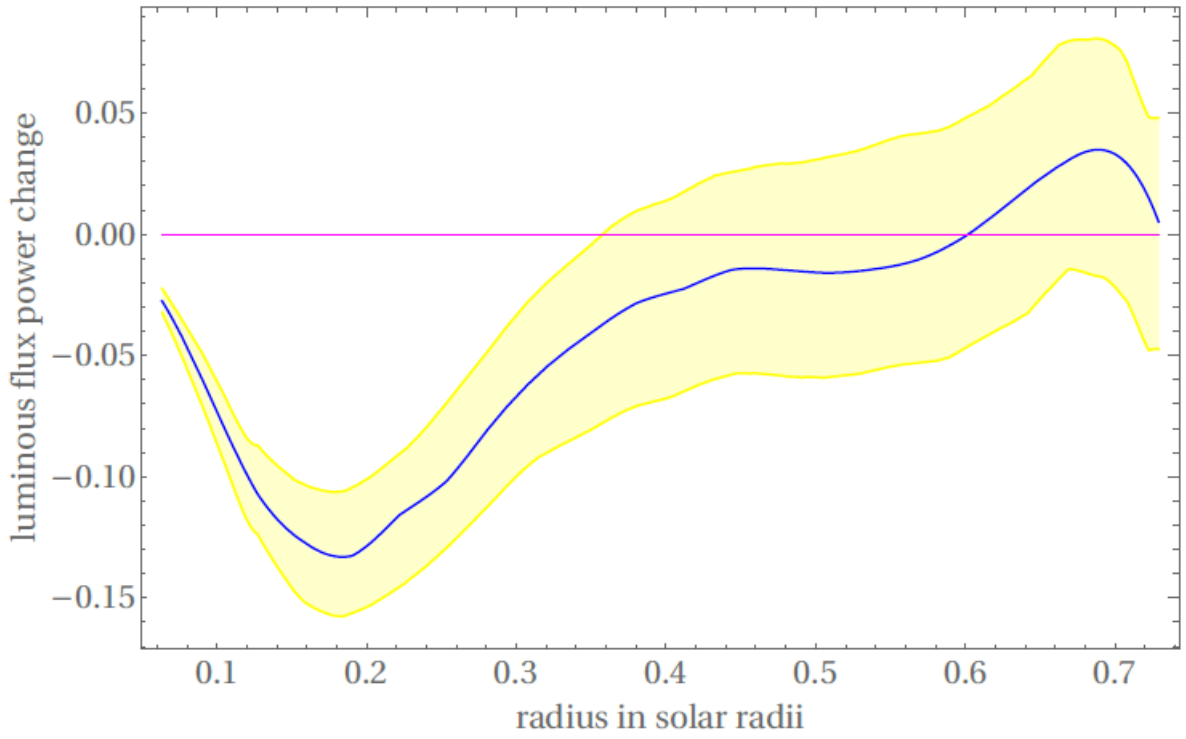

Figure 12: Additional power of luminous flux, which gives the helioseismological sound speed profile, as a function of radial coordinate inside the core and radiative zone, $\bar{\epsilon} = 0$, $C = -0.26$ [21]

8 Particle Physics Model [21]

One possible solution to the requirement of localized emission of energy at the boundary of radiative zone can be some resonant processes due to mixing of WISPS with photons. In particular, in case of hidden photons, the resonant conversion occurs whenever the thermal photon mass ω_{pl} is equal to the hidden photon mass $m_{\gamma'}$ or the hidden photon energy $\omega_{\gamma'}$, depending on the polarization of hidden photon.
Assumptions:

- Additional U(1)' gauge symmetry
- Mass of hidden photon $m_{\gamma'} \neq 0$.
- Mass mixing parameter is negligible compared to kinetic mixing

For resonant production of longitudinally polarized hidden photons, we need $\omega_{pl} \geq m_{gamma'}$, which is a large region inside the sun. These hidden photons will have some definite energy. For production of transversely polarized hidden photons, the resonant production will only occur in a thin spherical shell of width $\sim 10^{-4}\ R_{\odot}$.

Such a narrow region of resonant emission near the solar convective zone is exactly what we need. Using the condition $m_{gamma'} = \omega_{pl}(r = 0.7) = 12eV$. In this scenario, the resonant

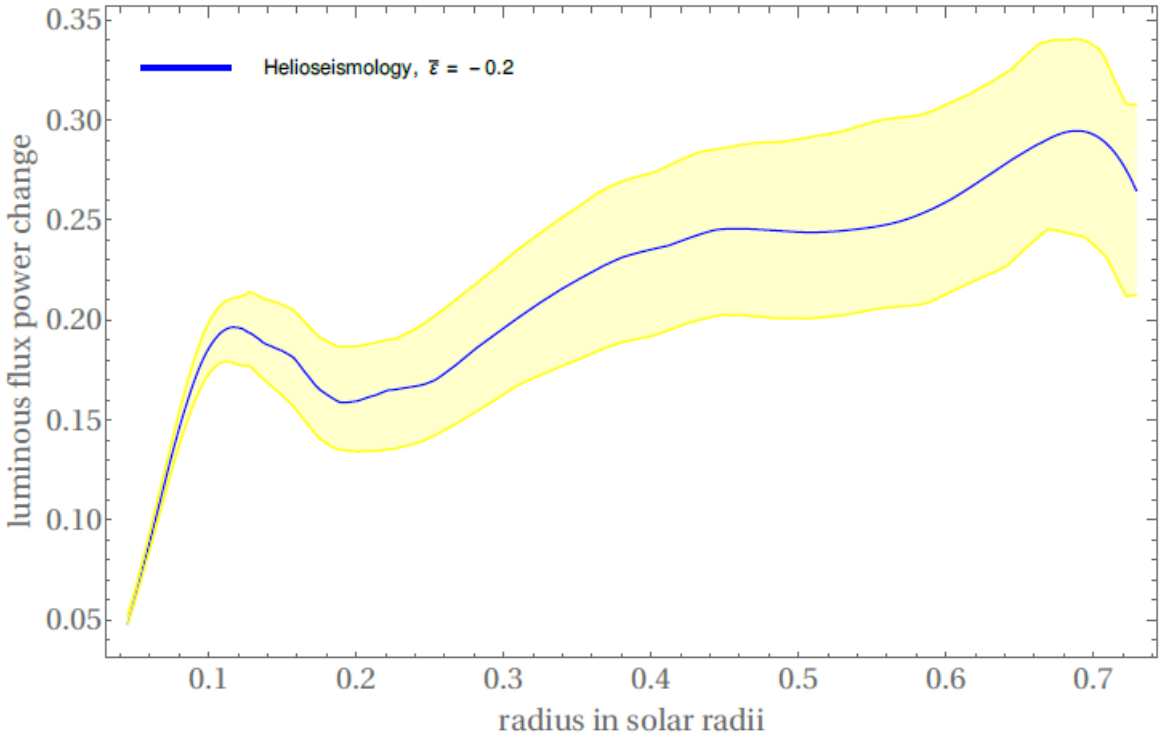

Figure 13: Required $(\delta l)_{add}$ to the power of luminous flux as a function of radial coordinate, $\bar{\epsilon} = -0.2$. This shows that additional loss of energy alone cannot be a solution to the solar abundance problem. [21]

production of longitudinally polarized hidden photons will be negligible.
To obtain the required $\Delta(\delta l) \simeq -0.26$, we need the kinetic mixing parameter $\chi \simeq 1.5 \times 10^{-13}$. These values do not contradict any existing laboratory or astrophysical constraints. However, we still need to ensure that the total energy loss $l_{loss} < 0.1$.

8.1 Millicharged particles

In case the energy scale of interaction and mass parts of Lagrangian (of the regular and hidden photons and their interaction with the electromagnetic field, various gauge fields and external currents (of both SM and hidden sector)) is larger than the hidden photon mass, the hidden sector particles acquire an effective millicharge.
Thus, we consider the decay of a hidden photon into two millicharged fermions ($2m_c < m'_\gamma$). In case the gauge coupling constant of the hidden sector, e', is $\gtrsim 10^{-6}$, the distance travelled by the hidden photon before its decay is negligibly small compared to the solar scale. This allows us to consider the region of production of millicharges in the sphere with great accuracy.

8.1.1 Capture of millicharged particles

The magnetic field inside the solar core is confined within it, since the solar core rotates as a rigid body. The boundary between the rigid rotation of the core and the highly non-uniform convective zone is very thin by the solar scale. Thus, we can consider the sun to have a toroidal magnetic field.
For the allowed values of millicharge (from astrphysics) $\varepsilon \lesssim 10^{-14} - 10^{-13}$, the Larmor radius of the millicharged particles is very small. This means the produced millicharges are captured within the magnetic fields in the solar core and are captured in the solar interior.

8.2 Solar Plasma Heating

For the millicharged particles to heat the solar plasma, the temperature of the gas of the dark sector particles needs to be higher than the solar plasma temperature ($\equiv 1$ keV. This is much higher than the average energy of the millicharged particles near the radiative boundary.
A proposed mechanism for the same is the presence of some stable heavy dark particles,gravitationally bound in the solar core.If these are charged under the hidden $U(1)'$ group and radiate dark photons, the required energy could be obtained. However, this has not been studied in detail. The main process contributing to the energy transfer from millicharged particles to solar plasma is the process of Coulomb scattering of millicharges on electrons. Considering the millicharged particles to be fermions, considering their low millicharge as a reason to approximate the interactions to be like compton scattering, and using some constraints developed by other authors studying the supernova SN1987, we get the following relation of energy transfer Q:

$$Q = 1.6\frac{\text{erg}}{\text{s.cm}^3} \times \left(\frac{\varepsilon}{7\times10^{-15}}\right)^2 \left(\frac{\omega_{pl}}{290\text{eV}}\right)^2 \left(\frac{T_c}{\text{keV}}\right)^3 \left[\frac{T}{T_c} - 1\right] K\left(\frac{4T_c^2}{\omega_{pl}^2}\right) \tag{62}$$

where K(a) as a function of radial coordinate is given in fig. 14
The final result of the above calculations requires the magnetic field in the solar interior to be higher than current constraints. However, the current constraints depend on pressure excess calculations. If the pressure exhibited by the millicharge gas or other hidden processes is high enough, the magnetic field constraints can be relaxed. The authors [21] do not provide estimates on the same.

9 Conclusions

- The Standard Solar Model and data obtained from helioseismic inversions differ and give rise to the solar abundance problem.
- The variation of luminosity in non-diffusive energy transfer vs SSM with helioseismic values is not enough to provide a constrained answer. The addition of factors from the hypothetical opacity shift solution helps give a constraint on the required energy transfer.

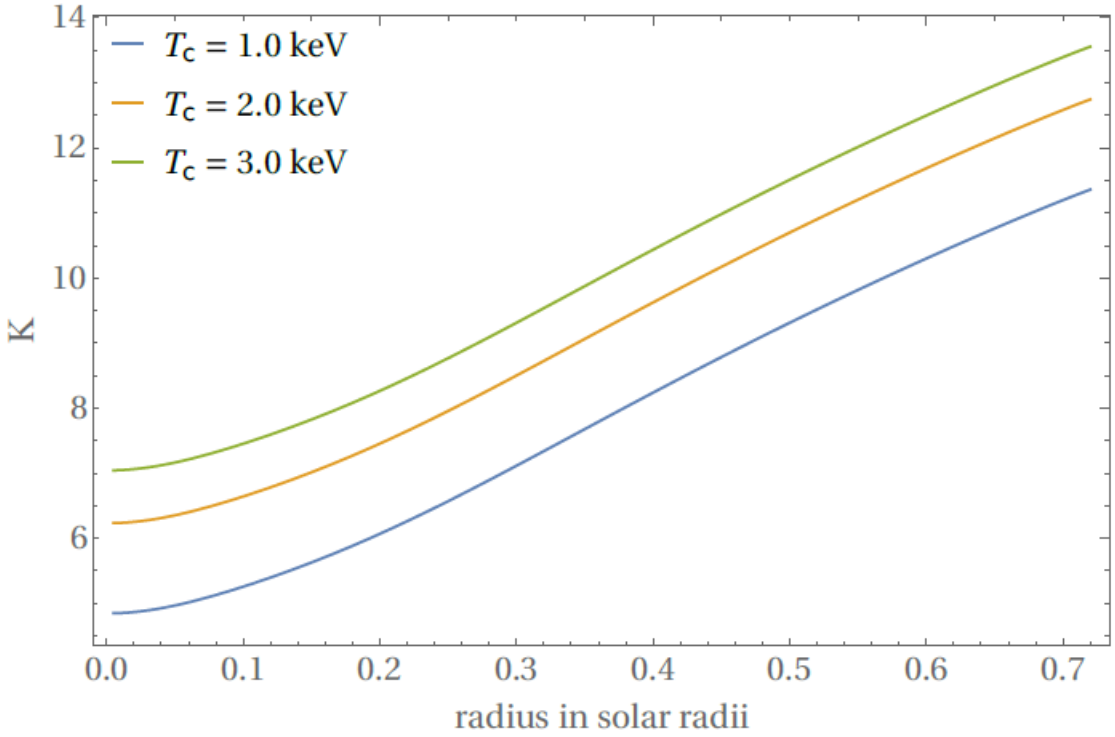

Figure 14: K(a) as a function of radial coordinate for the three values of temperature of the millicharged gas T_c [21]

- The results from this is production of energy at $r \in [0.1R_\odot, 0.3R_\odot]$ and deposition at radiation-convection boundary.
- This is being explained by the presence of millicharged particles. It has been shown in the paper that particles of certain properties can be captured by the Sun's magnetic field. These can heat the core enough for production of dark photons which can achieve the required variation of luminosity in the radiative zone (however, not in the convective zone).
- The paper [21] did not well explain any mechanism to maintain the temperature of the light dark fermions within the sun.

References

[1] E. Gupta, "Solar Physics and Implications to Exotic Particles", *MSc. Project Report*, Dec 2020.

[2] Jørgen Christensen-Dalsgaard, "Stellar Structure and Evolution", Institut for Fysik og Astronomi, Aarhus Universitet, Mar 2008.

[3] B. W. Carroll and D. A. Ostlie, "An Introduction to Modern Astrophysics." Cambridge University Press, sep 2017. [Online]. Available: https://doi.org/10.1017%2F9781108380980

[4] M. Bergemann and A. Serenelli, "Solar abundance problem," in Determination of Atmospheric Parameters of B-, A-, F- and G-Type Stars. Springer International Publishing, 2014, pp. 245–258. [Online]. Available: https://doi.org/10.1007%2F978-3-319-06956-2_21

[5] S. Basu and H. Antia, "Helioseismology and solar abundances," Physics Reports, vol. 457, no. 5-6, pp. 217–283, mar 2008. [Online]. Available: https://doi.org/10.1016%2Fj.physrep.2007.12.002

[6] S. Basu and W. J. Chaplin, "Asteroseismic Data Analysis", *Princeton Series in Observational Astronomy*. Revised, Mar 2017.

[7] Jørgen Christensen-Dalsgaard, "Stellar Oscillations", Institut for Fysik og Astronomi, Aarhus Universitet, May 2003.

[8] S. Basu, "Global seismology of the sun, "Living Reviews in Solar Physics, vol. 13, no. 1, aug 2016. [Online]. Available: https://doi.org/10.1007%2Fs41116-016-0003-4

[9] P. L. Pallé, Christensen-Dalsgaard, et al, "Helioseismology-Observations and SPace Missions", *olar and Stellar Astrophysics (astro-ph.SR)*, Feb, 2018. [Online] Available https://arxiv.org/abs/1802.00674

[10] N. Grevesse and A. Sauval, Space Science Reviews, vol. 85, no. 1/2, pp. 161–174, 1998. [Online]. Available: https://doi.org/10.1023%2Fa%3A1005161325181

[11] M. Asplund, N. Grevesse, A. J. Sauval, and P. Scott, "The chemical composition of the sun," Annual Review of Astronomy and Astrophysics, vol. 47, no. 1, pp. 481–522, sep 2009. [Online]. Available: https://doi.org/10.1146%2Fannurev.astro.46.060407.145222

[12] J. Christensen-Dalsgaard, M. P. D. Mauro, G. Houdek, and F. Pijpers, "On the opacity change required to compensate for the revised solar composition," Astronomy & Astrophysics, vol. 494, no. 1, pp. 205–208, dec 2008. [Online]. Available: https://doi.org/10.1051%2F0004-6361%3A200810170

[13] S. Vagnozzi, K. Freese, and T. H. Zurbuchen, "Solar models in light of new high metallicity measurements from solar wind data," The Astrophysical Journal, vol. 839, no. 1, p. 55, apr 2017. [Online]. Available: https://doi.org/10.3847%2F1538-4357%2Faa6931

[14] D. G. Cerdeño, J. H. Davis, M. Fairbairn, and A. C. Vincent, "CNO neutrino grand prix: the race to solve the solar metallicity problem," Journal of Cosmology and Astroparticle Physics, vol. 2018, no. 04, pp. 037–037, apr 2018. [Online]. Available: https://doi.org/10.1088%2F1475-7516%2F2018%2F04%2F037

[15] M. Agostini et al., "Sensitivity to neutrinos from the solar CNO cycle in Borexino," Eur. Phys. J. C, vol. 80, no. 11, p. 1091, 5 2020.

[16] D. O. Gough, "Anticipating the sun's heavy-element abundance," Monthly Notices of the Royal Astronomical Society: Letters, vol. 485, no. 1, pp. L114–L115, mar 2019. [Online]. Available: https://doi.org/10.1093%2Fmnrasl%2Fslz044

[17] N. Song, M. C. Gonzalez-Garcia, F. L. Villante, N. Vinyoles, and A. Serenelli, "Helioseismic and neutrino data-driven reconstruction of solar properties," Monthly Notices of the Royal Astronomical Society, vol. 477, no. 1, pp. 1397–1413, mar 2018. [Online]. Available: https://doi.org/10.1093%2Fmnras%2Fsty600

[18] A. Sokolov, "Generic energy transport solutions to the solar abundance problem—a hint of new physics," Journal of Cosmology and Astroparticle Physics, vol. 2020, no. 03, pp. 013–013, mar 2020. [Online]. Available: https://doi.org/10.1088%2F1475-7516%2F2020%2F03%2F013

[19] A. C. Vincent, A. Serenelli, and P. Scott, "Generalised form factor dark matter in the sun," Journal of Cosmology and Astroparticle Physics, vol. 2015, no. 08, pp. 040–040, aug 2015. [Online]. Available: https://doi.org/10.1088%2F1475-7516%2F2015%2F08%2F040

[20] A. C. Vincent, P. Scott, and A. Serenelli, "Possible indication of momentum-dependent asymmetric dark matter in the sun," Physical Review Letters, vol. 114, no. 8, feb 2015. [Online]. Available: https://doi.org/10.1103%2Fphysrevlett.114.081302

[21] Sokolov, Anton V. "Generic energy transport solutions to the solar abundance problem—a hint of new physics." Journal of Cosmology and Astroparticle Physics 2020.03 (2020): 013.

[22] Villante, F. L. "Constraints on the opacity profile of the sun from helioseismic observables and solar neutrino flux measurements." The Astrophysical Journal 724.1 (2010): 98.

[23] Villante, F. L. "Linear Solar Models: a simple tool to investigate the properties of solar interior." arXiv preprint arXiv:1001.2510 (2010).

[24] Chung, Moo Dalton, Kim Davidson, Richard. (2008). Tensor-Based Cortical Surface Morphometry via Weighted Spherical Harmonic Representation. IEEE transactions on medical imaging. Available: 27.1143-51.10.1109/TMI.2008.918338.

[25] A. Ayala, et al, "Constraining dark photon properties with Asteroseismology", *Monthly Notices of the Royal Astronomical Society*, vol. 491, no. 1, Jan 2020. [Online]. Available : https://academic.oup.com/mnras/article-abstract/491/1/409/5610237?redirectedFrom=fulltext

[26] B. E. J. Pagel, "Stellar and Solar Abundances", *Royal Greenwich Observatory*, vol. 15, 1973. [Online] Available: http://adsabs.harvard.edu/pdf/1973SSRv...15....1P